ISSN 1063-7710, Acoustical Physics, 2011, Vol. 57, No. 2, pp. 168–179. © Pleiades Publishing, Ltd., 2011.
Original Russian Text © V.A. Gordienko, N.V. Krasnopistsev, V.N. Nekrasov, V.N. Toropov, 2011, published in Akusticheskii Zhurnal, 2011, Vol. 57, No. 2, pp. 179–191.

OCEAN ACOUSTICS.
HYDROACOUSTICS

Localization of Sources on a Ship Hull Using Combined Receiver and High-Resolution Spectral Analysis

V. A. Gordienko[a], N. V. Krasnopistsev[b], V. N. Nekrasov[b], and V. N. Toropov[b]

[a] *Physical Faculty, Moscow State University, Moscow, 119991 Russia*
e-mail: vgord@list.ru

[b] *FSUE National Research Institute for Physical Technical and Radio Engineering Measurements, Mendeleevo, Moscow oblast, 141570 Russia*

Received May 13, 2009

Abstract—The fundamental possibility of application of a single combined receiving system based on a three-component vector receiver for solution of problems of estimation of direction and localization of individual sources on a ship hull, source membership selection, and more reliable estimation of source signal levels is demonstrated. It is proposed to use high-frequency resolution methods of sonographic analysis (spectral–time representation) of projections of the acoustic power flux vector for spatial resolution of sources that provide a higher signal-to-noise level at the output of the processing system.

DOI: 10.1134/S1063771011020060

1. INTRODUCTION

The problem of localization and measurement of levels of low-frequency, low-level signal sources at present is one of the topical problems of modern hydroacoustics. Usually either a "strip" of single hydrophones [1, 2] or antenna arrays of different designs [3] are used for this purpose. One class of these problems, localization of low-power emission sources on a ship's hull, assumes the presence of good diagnostic tools for analysis of the noise source and estimation of its location on the hull and emission level for providing noise reduction of a particular sea object. The problem of obtaining an acoustic image is extremely difficult, since the required spatial source resolution at low frequencies is usually several times smaller than the acoustic wavelength. This is to a large extent the reason why the application of extended multielement antennas based on hydrophones often possesses low efficiency, especially at low signal-to-noise ratios. As a result, a tendency toward growing interest in compact hydroacoustic systems, including acoustic pressure receivers and vector receivers [4, 5], has been observed recently in our country and abroad. Compact receiving systems in which a nondirectional hydrophone and vector receiver are combined in one frame and have one phase center are usually called combined receiving systems or combined receivers.

Paper [6] presents results of testing capabilities of antenna array consisting of five vector receivers situated at a distance of 10 cm from each other in the vertical direction in determination of the position and intensity of sources on the hull of a submarine at the SEAFAC stationary hydroacoustic testing area of the US Navy in Behm (Alaska, not far from the village of Ketchikan). Localization of sources on a submarine hull was achieved by comparison of responses of different channels of separate vector receivers on the assumption that there exists only one source onboard in the frequency interval of interest. If several sources were present, narrow beam directional diagram was formed by corresponding choice of the weighting vector in the algorithm of beam multiplicative processing.

In our opinion, this approach cannot be considered optimal for low frequencies. Therefore, in our studies we use a single combined receiving system or combined receiver, or, which is better, two combined receiving systems at a rather large distance from each other and then use the triangulation method for increasing the source localization accuracy. High-frequency resolution methods of spectral–time representation (sonographic analysis) of projections of acoustic power fluxes are used for spatial resolution of sources; these methods make it possible to increase the signal-to-noise ratio at the output of the processing system.

2. GOALS AND METHOD FOR SOURCE LOCALIZATION USING VECTOR RECEIVER

The measurements were performed for experimental verification of the possibility of application of vector receivers for localization and more reliable estimation of levels of separate sources due to statistical spatial filtering of acoustic power flux vector in conditions of water areas of stationary sea test sites in the case of a motionless ship with operating mechanisms near the berth or the coastline of an industrial zone.

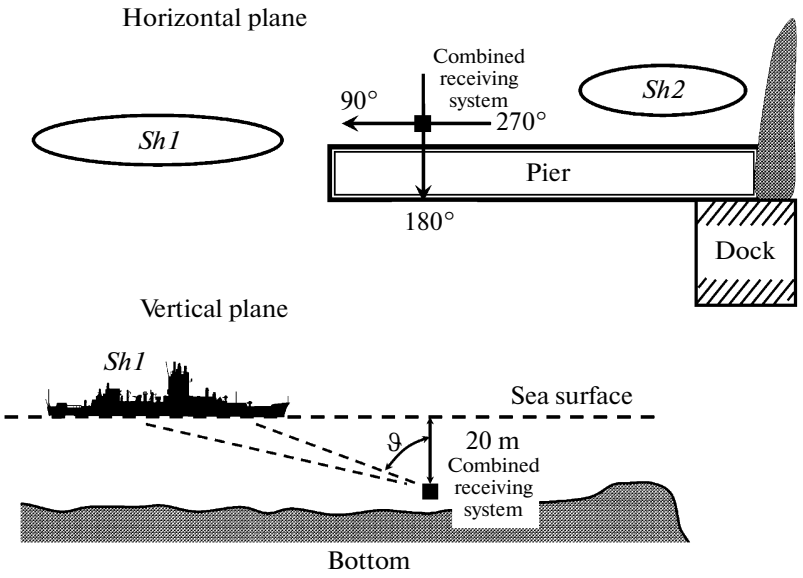

Fig. 1. Geometry of measurements in (upper) horizontal and (lower) vertical planes.

A combined receiving system containing a three-component vector receiver with a working frequency range of 5–1000 Hz and an acoustic pressure receiver placed in a dome of special design was used in experiments. The geometry of location of the combined receiving system and potential noise sources in the horizontal and vertical planes is shown in Fig. 1. The studied ship *Sh1* with operating main mechanisms was anchored not far from a pier. Another ship (*Sh2*) was moored to this pier. The dock with operating mechanisms was situated in the immediate neighborhood on the other side of the pier. The combined receiving system was at a distance of about 25 m in the horizontal plane from the ship bow, 1 m from the water area bottom at a depth of approximately 20 m. The horizontal axis of the ship was directed practically toward the combined receiving system (Fig. 1). Such suboptimal geometry of the mutual position of the receiving system and the ship in the framework of the described experiment prevented distinguishing individual sources of the ship *Sh1* in the azimuthal plane. In this case the possibility of separation of these sources was provided only in the vertical plane taking into account the difference of the submergence depth of the noise sources and the combined receiving system. In principle, for reliable source separation, it is necessary to place the combined receiving system in such a way that one of the ship boards is observed from the side, as described, for example, in [6]. The axis of one of the vector receiver channels was oriented in the vertical direction. The spatial orientation of horizontal channels of the vector receiver was matched by measurement of the angle of signal arrival from a localized acoustic source; a motorboat tacking along the known controlled trajectory near the combined receiving system was used as this acoustic source.

The acoustic power flux vector is usually determined by the averaged over the period T (or the time τ multiple or much larger than the period) value of the Umov vector [4],

$$\mathbf{W}_\mathrm{R} = \overline{\mathbf{I}(t)} = \frac{1}{\tau}\int_0^\tau \mathbf{I}(t)dt \equiv \frac{1}{\tau}\int_0^\tau P(t)\mathbf{V}(t)dt.$$

Hereinafter, the symbol "$\overline{\ldots}$" means time averaging. The projection $W_{\mathrm{R}r}$ of the vector $\mathbf{W}_\mathrm{R}$ on the direction $\mathbf{r}$ characterized by the projection of the oscillation velocity $V_r(t)$ is determined as $W_{\mathrm{R}r} = \frac{1}{\tau}\int_0^\tau P(t)V_r(t)dt$ and for the narrow-band (quasiharmonic) signal with the average frequency f as

$$W_{\mathrm{R}r}(f) = \frac{1}{2}P_0V_{0r}\cos(\Delta\varphi_{PV})$$

$$= \frac{1}{2}\mathrm{Re}(P^*V_r) = \frac{1}{4}(PV_r^* + P^*V_r),$$

where $\Delta\varphi_{PV}$ is the phase difference between the pressure and projection of oscillation velocity with the amplitudes P_0 and V_{0r}, respectively, and the symbol "*" denotes a complex conjugate quantity.

It has been noted earlier [4, 7] that a single combined receiving system formally does not make it possible to calculate the spatial spectrum with the wave vector $\mathbf{k}(\omega, \mathbf{r})$, but, at the same time, allows it to be estimated using measurements performed in a spatial region much smaller than the wavelength. The algo-

rithm of determination of the direction toward the source used in this study was described in detail in [4]. This algorithm is based on statistical analysis of spatial distribution of the acoustic power flux vector $\mathbf{W}_R(f, t)$. This algorithm increases the noise resistance of the receiving system by 10...20 dB (determined mainly by statistical specific features due to the formation of acoustic power flux vector of the noise field and local sources in the sea area [8]) and uses well-known relations between the values of projections of the vector $\mathbf{W}_R(f, t)$ and the direction of arrival of the wave energy. It is known that, within a unit sample with the length τ_0 for each frequency subrange δf_i, the azimuthal φ_i and polar ϑ_i angles of signal arrival in the horizontal and vertical planes and the intensity I_i of this signal can be determined from the analyzed range Δf; the signal intensity represents the absolute value of acoustic power flux vector in the direction determined by the angles φ_i and ϑ_i,

$$\tan\varphi_i = \frac{W_{Ryi}}{W_{Rxi}}, \quad \tan\vartheta_i = \frac{W_{Rzi}}{\sqrt{W_{Rxi}^2 + W_{Ryi}^2}},$$
$$I_i(\varphi_i) = \sqrt{W_{Rxi}^2 + W_{Ryi}^2}, \qquad (1)$$
$$I_i(\varphi_i, \vartheta_i) = \sqrt{W_{Rxi}^2 + W_{Ryi}^2 + W_{Rzi}^2}.$$

The essence of the approach used below is as follows. The whole range of analyzed angles is separated into M sectors, for example, for the planar case of the horizontal plane $M = 360/\Delta\varphi_0$, where $\Delta\varphi_0$ is the chosen spatial resolution. For the given frequency band $\Delta f = \sum_{i=1}^{m} \delta f_i$ consisting of the set of m discrete frequency intervals with the band δf_i each (for example, the frequency resolution of fast Fourier transform or transmission band of the narrow-band filter), the discrete set of values (array) $I(\varphi_n)$ for the sample q is calculated according to the algorithm

$$I_q(\varphi_n) = \sum_{i=1}^{m} I_{qi}\left[f_i, (n-1)\Delta\varphi_0 \le \varphi_i < n\Delta\varphi_0\right], \qquad (2)$$

where n takes values from 1 to M. The result can be reduced to a band of 1 Hz by division of the obtained values of $I_q(\varphi_n)$ by $\sum_{i=1}^{m} \delta f_i$ if necessary (if it does not contradict the formulated problem). The reduction of the results to the 1/3-octave band was performed by weighted summing using a specially developed code. Subsequently, the next sample $(q + 1)$ is considered and the procedure is repeated, yielding the array of values of $I_{q+1}(\varphi_n)$ for a following time instant larger than the previous one by $\Delta\tau$, which is usually several times smaller than the length of the analyzed fast Fourier transform sample.

If, for obtaining the values of acoustic power flux projections, for example, on X and Y axes a segment of signal record with the length $t_{sm} > \tau_0$ multiple to $\Delta\tau$ is chosen for some τ_0, for each frequency on the record length t_{sm} $N_{sm} = t_{sm}/\Delta\tau$ counts of the angle φ and intensity $I(\varphi)$, i.e., a total of $N_{sm}m$ values of $I(\varphi)$, can be obtained. For reducing fluctuations, a histogram of $I(\varphi_n)$ distribution in the analyzed frequency band Δf averaged over N_{sm} counts in each of M angular sectors is constructed based on the obtained data. In this case, common averaging matched, for example, with the length of the analyzed record fragment t_{sm} can be used. However, if the number N of counts (samples) is not known a priori, or in the case of real-time operation, or if a sonogram or 3D diagram is constructed at the output of the data-processing system, it is optimal (according to recommendations of experts of the company Bruel and Kjaer [9, 10]) to consider the so-called "logarithmic" averaging, which yields rapid convergence to the final result even for the number of counts $q = N < N_{sm}$,

$$I(\varphi_n) = \frac{(N_{sm} - 2) I_{q-1}(\varphi_n) + 2I_q(\varphi_n)}{N_{sm}}. \qquad (3)$$

Here, $I(\varphi_n)$ is the current averaged value of intensity in the angular interval φ_n for which $(n-1)\Delta\varphi_0 \le \varphi < n\Delta\varphi_0$, $I_q(\varphi_n)$ is the result of determination of the value of intensity for the sample with the number q using formula (2), $I_{q-1}(\varphi_n)$ is the result of averaging using formula (3) at the previous step. The value of N_{sm} is usually chosen from the conditions of "reasonable" stationary character for the time interval t_{sm}.

In order to increase the number of independent unit counts, narrow-band spectral analysis is usually used (for example, by choosing the sample τ_0 for fast Fourier transform to be large as possible) and intensity is reduced to the given frequency–angular range by summing the intensities in neighboring frequency bands of the signal. However, in this case, for signals with a low signal-to-noise ratio at the input, problems can occur; these problems will be discussed below.

If $N_{sm}m \gg M$, distribution (3) at the step $q \ge N_{sm}$ can be considered as the ***quasi-spatial spectrum of acoustic signal with respect to the acoustic power flux*** in the horizontal plane for the time interval t_{sm}. In the case of absence of high-power localized sources in the water area and absence of high-level background noise arriving along the vertical coordinate (this condition is most often satisfied), in the first approximation, it may be close to the spatial spectrum obtained using the horizontal linear antenna. If the oscillation velocity is expressed in terms of equivalent units of acoustic pressure of a plane acoustic wave (i.e., ρcV is considered instead of V, where ρc is the wave resistance of the medium), the dimensionalities of I and P^2 coincide,

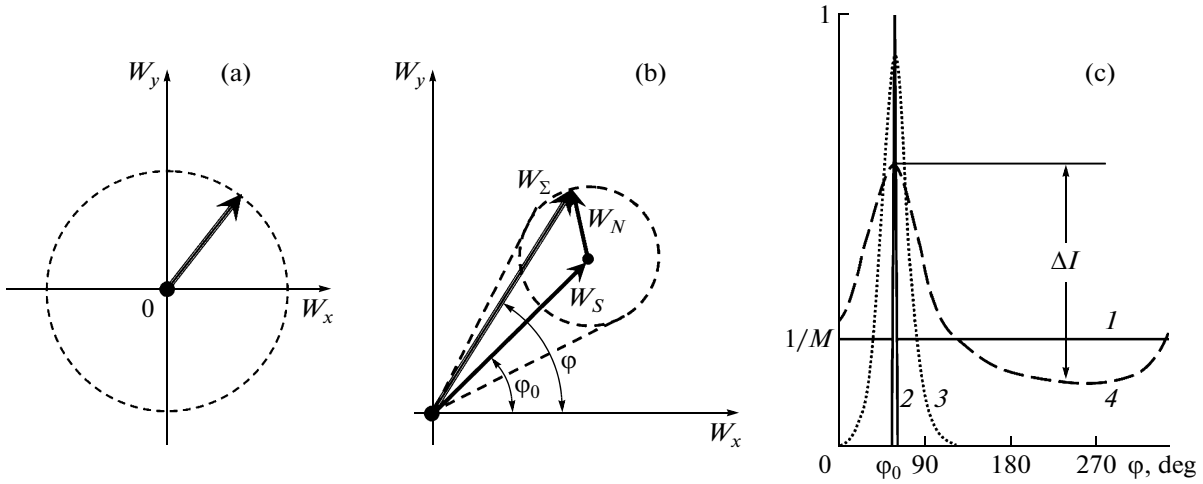

Fig. 2. On formation of spatial statistical distribution of acoustic power flux vector $\mathbf{W}_R$: (a) noise isotropic in horizontal plane; (b) possible angular positions φ in the horizontal plane of the total acoustic power flux vector $\mathbf{W}_\Sigma$ in the presence of a local source forming acoustic power flux $\mathbf{W}_S$ in the direction φ_0 and isotropic noise $\mathbf{W}_N$ ($W_N < W_S$) in the water area; (c) approximate dependences of the distribution $I(\varphi)$ normalized to P^2 for several typical cases: (*1*) isotropic noise without a local source, (*2*) local source in the absence of noise, (*3*) W_S level is much higher than noise W_N level; and (*4*) $W_S \lesssim W_N$.

and their numerical values can be compared. In this case for the water layer with the impedance boundary, according to [4], the following condition should be satisfied:

$$\sum_{n=1}^{M} I(\varphi_n) \equiv I_{\Sigma I} \approx P^2. \quad (4)$$

At first sight it seems that the application of an acoustic power flux receiver formally makes it possible to obtain any spatial resolution. However, it should be taken into account that, unlike antenna arrays, determination of spatial distribution of intensity based on combined processing of the signals $P(\mathbf{r}, t)$ and $\mathbf{V}(\mathbf{r}, t)$ assumes signal expansion in the spatial domain over the nonorthogonal basis [4]. It should also be noted that the histogram represents the result of statistical signal processing and reflects the real noise anisotropy in the water area only in the absence of high-power angularly localized sources. In this case obtained results can be interpreted as the ***spatial noise spectrum in the water area***. In the presence of a high-power localized source in the water area, the spatial spectrum is distorted. This is due to the fact that the direction of "instantaneous" value of the vector $\mathbf{W}_\Sigma$, the absolute value of which is determined by the value of $I(\varphi)$ introduced above at each time instant is determined as the sum of relatively spatially stable vector $\mathbf{W}_S$ generated by the localized source and the vector $\mathbf{W}_N$ of the field of self noise of the water area distributed according to some random law (Fig. 2),

$$I(\varphi) = |\mathbf{W}_\Sigma| = |\mathbf{W}_S + \mathbf{W}_N|.$$

Indeed, let us consider the behavior of the acoustic power flux vector formed by the localized source in the presence of noise isotropic in the horizontal plane. The noise signal intensity in the angular sector $\Delta\varphi$ in the absence of a localized source in the case of processing according to the algorithm described above is determined by the value of P^2/M (Fig. 2c, dependence *1*). If there exists a localized source only, it creates acoustic power flux at an observation point that is not zero on average and is concentrated in the angular interval determined by expressions (1) (Fig. 2c, dependence *2*). Therefore, by observing the acoustic field at one point, the conclusion that there is a direction toward the source (***which is the essence of the direction-finding problem***), rather than the spatial noise spectrum, can be drawn. In the general case (in the presence of noise and localized source), the probability density distribution of the acoustic power flux vector for the localized source at the background of isotropic noise is described using the MacDonalds function [11]. The true direction-finding for the localized source in this case can be solved by additional processing of the profile of the envelope $I(\varphi)$. The approximate form of the distribution $I(\varphi)$ for finite signal-to-noise ratios is shown in Fig. 2c (dependences *3* and *4*). As the signal-to-noise ratio decreases, the direction-finding variance increases and, finally, signal excess over background noise can become comparable with the fluctuation component of the histogram. If other localized noise sources are present in the water area, the profile of the dependence $I(\varphi)$ is more complex.

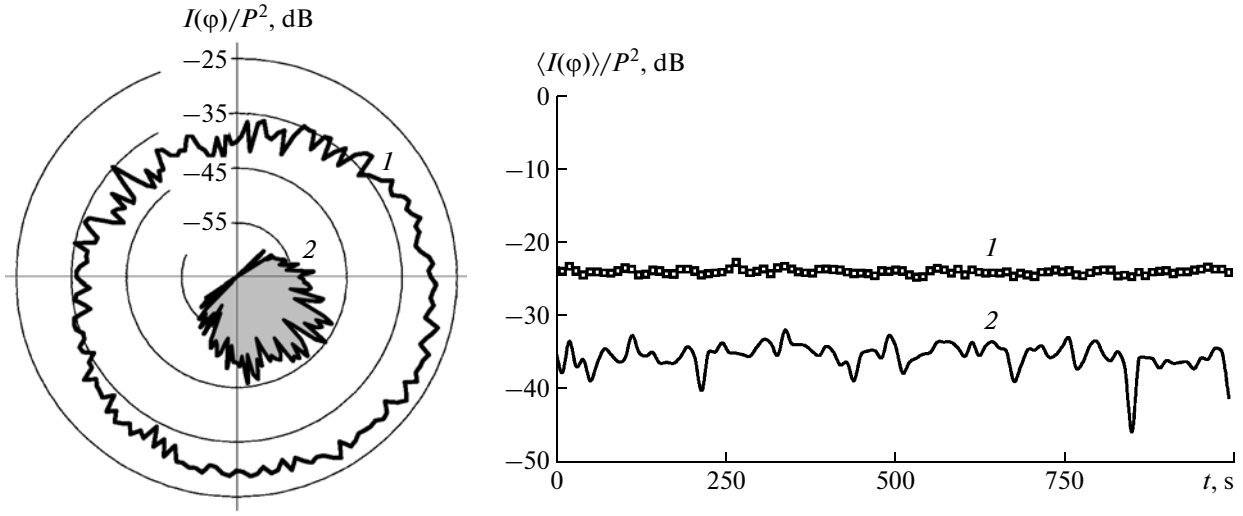

Fig. 3. Spatial distribution $I(\varphi)$ normalized to P^2 and averaged over the angle φ distribution $\langle I(\varphi)\rangle$ of noise intensity in the Water sea area in a frequency range of 78...315 Hz obtained using (*1*) algorithm I and (*2*) algorithm II as functions of time.

There exists another (second) approach (let us call it **algorithm II**, unlike **algorithm I** described above), the main part of which is the same as that of the algorithm described above. The difference is in the histogram construction method. Namely, within a separate sample, each angular cell with the number n characterized by the average value of the direction-finding angle φ_n contains intensities determined, for example, from the condition

$$I(\varphi_n) \Rightarrow \hat{I}(\varphi_n) = \left(1/2\right) \times \left\{\left[I\left(\varphi_n\right) - I\left(180^\circ + \varphi_n\right)\right] + \left|I\left(\varphi_n\right) - I\left(180^\circ + \varphi_n\right)\right|\right\}.$$

In this case the ***isotropic component of water area noise decreases rather fast already for small averaging times*** and only relatively stable (stationary) in space and time anisotropic components of noise sources are left. This algorithm can be efficiently used for separation of the source of weak signals on the background of water area noise on the condition that the frequency and angular characteristics of the separated source and stationary components of the noise field do not coincide. The best effect should be obtained if the water area noise is close to isotropic. In this case the noise resistance of the receiver recording the acoustic power flux vector can essentially exceed 20 dB [8].

Obviously, $I(\varphi)$ levels obtained using algorithms I and II coincide only for localized signal sources stationary with respect to direction-finding during processing. Usually different levels are obtained for the field of distributed noise sources. Algorithm II determines the level of the anisotropic component of acoustic power flux taking into account fluctuations (depending on averaging time); therefore, if the averaging time τ increases, it decreases to this level according to classical rules. It can be easily shown that, for algorithm II, unlike (4), the following inequality is always satisfied: $I_{\Sigma II} = \sum_{n=1}^{M} I(\varphi_n) < P^2$. Concerning algorithm I, it contains information on the amplitude–spatial (with account of fluctuations) intensity distribution and depends on statistical characteristics of the studied noise field. Therefore, it was already indicated above that for this algorithm, due to the specific features of formation of the spatial distribution of the vector $\mathbf{W}_R$, the angular dependence $I(\varphi_n)$ does not necessarily coincide with that determined using the extended antenna array. Although, in principle, if there are not more than one or two localized sources in the water area, it can be reconstructed using relatively simple processing algorithms.

The example of processing data of a full-scale experiment in the horizontal plane for the White Sea area (depth of about 300 m) according to algorithms I and II in the absence of visible localized sources in the area is shown in Fig. 3. The angular distribution $I(\varphi)$ normalized to the integral value of P^2 for $M = 360$ (angular resolution of 1°) constructed according to algorithm I corresponds to the statistical spatial resolution of the vector $\mathbf{W}_R$ of the area noise at the place of location of the receiving system in the horizontal plane. For the normalized values of $I(\varphi)$ shown in the figure, the condition $\sum_{n=1}^{360}\left(I(\varphi_n)/P^2\right) = 1$ is well satisfied, i.e., the integral intensity level is equal to P^2.

The dependence $I(\varphi)$ constructed according to algorithm II reflects the spatial distribution of a relatively stable in the horizontal plane anisotropic component of acoustic power flux vector for the noise field the integral level for this region of which is lower than P^2 by $\gamma_a = 13...15$ dB. This means that, according to

formal criteria, a single combined receiving device can in principle determine the direction to relatively weak localized sources for which the signal-to-noise ratio in the pressure channel is much lower than unity on the background of moderately isotropic noise fields based on measurement of acoustic field characteristics at one point.

However, upon estimation of potential capabilities of separation of weak signals on the background of the water area noise some problems arise. Thus, for example, for the situation described above the deterministic source with the signal level at the output of a single non-directional hydrophone equal to the noise level of the water area should exceed the level of acoustic power flux in the angular sector of interest by the value $\gamma_a = 13...15$ dB. However, that is not so. Unlike the antenna array for which the value of γ_a characterizes its noise resistance in the given angular sector, the value of ΔI of excess of the localized source signal with respect to the water area noise level (Fig. 2c) depends on a number of factors. The main factor is the signal-to-noise ratio for the acoustic power flux. Unlike the antenna array, the angular spectrum of energy arrival from the localized source determined using the above algorithms is rather broad. This is connected with essential spatial and temporal fluctuations of the total registered vector $\mathbf{W}_S + \mathbf{W}_N$ formed with participation of the localized source. Obviously, as was noted above, the direction-finding variance essentially depends on the ratio $|\mathbf{W}_S|/|\mathbf{W}_N|$. The latter, of course, makes the difference of direction-finding using the combined receiving system and the antenna array. Therefore, usually additional processing of the $I(\varphi)$ envelope is required for determination of the true direction toward the source with a given accuracy, as well as for determination of the true signal level of this source.

HIGH-RESOLUTION SPECTRAL ANALYSIS

Further improvement of the signal-to-noise ratio is performed due to application of algorithms of high frequency resolution spectral analysis based on methods of time–frequency signal transformations described in [7, 12]. These algorithms, as a rule, provide spatial separation of sources of discrete components of signals generated by different objects in the same frequency range.

Indeed, if the band for spectral analysis decreases, the direction-finding variance can be reduced (and therefore, the reliability of separation of the signal from the localized source on the background of ambient noise can be increased) due to increasing the ratio $|\mathbf{W}_S|/|\mathbf{W}_N|$ (Fig. 4) and the fluctuation component can be reduced due to increasing statistics. However, in many practical cases, especially for moving objects, the averaging time often cannot be essentially increased. Therefore, practically the only way of simultaneous satisfaction of both conditions is the

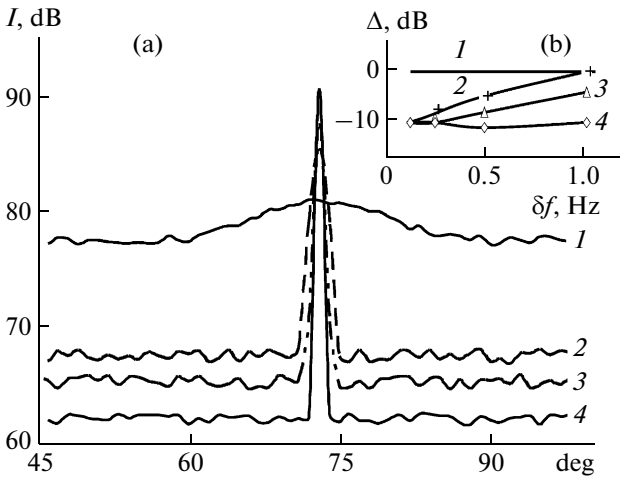

Fig. 4. Profiles of dependence $I(\varphi)$ (a) for nonfluctuating with respect to the frequency harmonic signal at different frequency resolution ((*1*) 1, (*2*) 0.1, (*3*) 0.06, (*4*) 0.03 Hz); (b) estimation of the value of Δ of $I_{\max}(\varphi)$ reduction with respect to registered non-fluctuating harmonic signal for different signal frequency fluctuation ((*1*) 0.01, (*2*) 0.5, (*3*) 1, (*4*) 3 Hz).

larger number of analyzed frequency bands, i.e., higher-frequency resolution of spectral analysis. This method, in most practical cases, provides spatial separation of two and more real broad-band signal sources operating in intersecting frequency bands. The latter is usually connected with the possibility of separation of the discrete noise component from most sea objects, which always exist.

However, high-frequency resolution imposes certain constraints on the capabilities of separation of weak signals on the background of ambient noise of the water area. Two problems should be solved in this case. The first one is connected with the necessity of increasing the array of processed data in the case of narrow-band analysis. It is known that if standard fast Fourier transform algorithms are used the width of the frequency band for analysis is inverse proportional to the sample length. This means that, while for operation in a frequency range of 0...1000 Hz for a frequency resolution of 1 Hz, a sample with a volume of approximately 3000–4000 counts per each channel is required, in the case of a frequency resolution of 0.05 Hz, the sample volume can reach 80000 counts. The second problem is the presence of frequency fluctuations of the signal both due to unstable operation of emitting mechanisms of the object, signal propagation fluctuations, and the Doppler effect if the studied object moves.

The first problem is solved in a simple way. For reducing the volume of the analyzed sample, so-called digital quadrature and low-frequency filtering with subsampling can be used. These are usually designated for preliminary signal processing necessary for realiza-

tion of high-frequency resolution algorithms of spectral and sonographic analysis. Quadrature signal filtering (complex demodulation) is the method used in signal processing problems in which some spectral region of the signal inside the frequency interval $\{f_c; f_c + f_n\}$ is useful for the solved problem [13]. It is realized by multiplying the initial signal $U(i\Delta t)$ discretely digitized with the quantization frequency $f_d = 1/\Delta t$ (Δt is the initial quantization time interval and i is the count number) by the complex exponential function $\exp(j2\pi f_c i\Delta t)$. Here, f_c is the lower frequency of the analyzed frequency interval, $j = \sqrt{-1}$. As a result of multiplication of the signal $U(i\Delta t)$ by the complex exponential function, the neighborhood of its spectrum with the center determined by the frequency f_c of the exponential function is shifted toward zero frequency. Then the signal is filtered using the low-frequency filter with the cutoff frequency f_n (boundary of nontransmission frequency of the low-frequency filter); as a result, only the spectral segment of interest is preserved in the frequency interval $\{f_c, f_c + f_n\}$. The thus-formed complex signal is usually called the complex envelope. Then, according to the width of the band of low-frequency filtering (Nyquist condition), the new quantization frequency f_D of the complex envelope is chosen, $f_D \geq 2f_n$. The choice of f_D is realized by subsampling of counts of quadrature components of the signal at the outputs of low-frequency filters. The result of quadrature filtering with subsampling is a complex signal in which spectral characteristics of the original signal in the filtering interval $\{f_c; f_c + f_n\}$ realized in a frequency band from 0 to f_n are preserved. Then high-frequency resolution spectral analysis is performed based on methods of time–frequency signal transformations [12, 13].

Three algorithms of such transformations are considered most often: time–frequency representation based on the fast Fourier transform (F algorithm), time–frequency Wigner representation (W algorithm), and time–frequency representation using the compensating function of signal frequency variation with linear frequency modulation (Q algorithm). Each of these signal representation types possesses positive and negative properties. This prevents making an unambiguous choice of one of them.

The main parameter of high-frequency resolution algorithms is the effective width of the weighting function $h(t)$ determining the effective width of the sliding time window used in spectral analysis for reducing side lobes [14]. The choice of effective width depends on the high-frequency resolution algorithm and the analyzed signal.

The time–frequency representation usually is the sequence of Fourier spectra calculated for the sequence of segments (as a rule, overlapping) of the signal $U(t)$ with the sliding time window $h(t)$ of effective width ΔT_{eff}. This representation possesses rather good noise stability. The noise level for this representation is known [15] to decrease inverse proportional to the effective width of the window ΔT_{eff}, while the intensity of the narrow-band peak corresponding to the signal stays the same and, therefore, the signal-to-noise ratio increases.

However, possible changes of frequencies of discrete components on the window time interval result in spectrum distortion (smearing). In this case frequency components of discrete component spectrum are manifested in several frequency bands that result in worsening of the signal-to-noise ratio at the output and makes further reduction of the interval for frequency analysis inefficient. Figure 4 shows the results of a model experiment on determination of the histogram $I(\varphi)$ (angular resolution of 1°) for the harmonic signal with a frequency of 230 Hz on the background of isotropic in the horizontal plane noise with a close to unity signal-to-noise ratio in the pressure channel. Spectral analysis with different frequency resolution δf was used. The dependences in Fig. 4a correspond to a signal that does not fluctuate with respect to frequency for the frequency resolution δf equal to 1 (curve *1*), 0.1 (curve *2*), 0.06 (curve *3*), and 0.03 Hz (curve *4*). Figure 4b shows the results of estimation of the value of Δ characterizing the reduction of the value of $I_{\max}(\varphi)$ in the direction toward the signal source for different frequency resolution δf of standard fast Fourier transform for different frequency fluctuation of the signal of localized source with respect to the value of $I_{\max}(\varphi)$ for a nonfluctuating signal. It can be seen that, for the frequency-unstable signal, as early as with a frequency analysis band of 0.1 Hz, up to 10 dB can be "lost" in the signal-to-noise ratio. If the parameter α with the meaning of variation rate of the instantaneous frequency of useful narrow-band signal ($\omega = \omega_0 + \alpha t$) is introduced, for the window width ΔT_{eff} larger than $(2\pi/\alpha)^{1/2}$ the signal intensity drops inversely proportionally to its width, i.e., the signal-to-noise ratio does not further grow. In this sense the window width $\Delta T_{\text{eff}} = \left(2\pi/\alpha\right)^{1/2}$ for F algorithm should be considered optimal.

For the Wigner distribution at finite time intervals with the sliding time window $h(t, \omega)$, the trajectory of frequency–time track of linear-frequency-modulated signal on the time–frequency plane is reproduced practically without errors, unlike Fourier transform. This distribution with the sliding time window can be used to separate (nonparametric approximation) trajectories of frequency tracks of multicomponent signals on the time–frequency plane, which vary practically according to an arbitrary law. With decreasing

efficient size of the time window, the analysis resolution obviously decreases.

For tonal sources moving in a medium, it was proposed in [16] to calculate the signal spectrum observed for the nonstationary signal given on the interval [0, T] as a function of two variables $S(\omega, \alpha)$, where, similar to above, α is the parameter with the meaning of variation rate of instantaneous frequency. The algorithm for spectrum estimation (Q algorithm) consists in searching sample functions with respect to the parameter α and choosing effective length of integration interval T for achieving a compromise between the resolution, bias errors due to deviation of the law of variation of instantaneous frequency from linear, and noise resistance. This algorithm possesses high noise stability, as compared to the algorithm based on Wigner transformation. The main disadvantage of this algorithm is the necessity of a priori finding the compromise between the length of the time interval of the sample function and the required resolution in the case of essentially "curvilinear" trajectories of frequency–time tracks and the necessity of a rather large search for the parameters of the sample function.

For the same time window width, the frequency resolutions of the considered algorithms for the stationary case ($\alpha = 0$) are connected as follows: $\Delta\omega_Q = 2\Delta\omega_F = 4\Delta\omega_W$.. For nonstationary signals this relation is more complex. A specific feature of W and Q algorithms is that there does not exist an optimal window for nonstationary signals since, with increasing window width, both frequency $\left(\Delta\omega \sim 1/T\right)$ and time $\left(\Delta T \sim 1/(\alpha T)\right)$ resolutions of these algorithms increase. In this case the amplitude of the linear-frequency-modulated signal in the sonogram is retained and the noise level decreases with increasing window width. However, degrees of noise suppression in these algorithms differ.

For W sonograms the estimation of the noise level σ^2 can be expressed by a relation the form of which is similar to that for the noise level in the case of the mutual correlation method of estimation of the level of narrow-band signal [15]; $\sigma_W^2 \sim \dfrac{A^2\sigma_\eta^2}{T} + \dfrac{\sigma_\eta^4}{T}$ (σ_η^2 is the noise level in the original signal). For Q sonograms $\sigma_\eta^2 \sim 1/\ln(T)$, i.e., in the latter case, the noise level in the sonogram decreases much more slowly with increasing window length [12]. Obviously, in the case of a nonlinear time dependence of the frequency components of the signal, the estimates of instantaneous frequency amplitude become shifted.

Figure 5 shows the obtained sonograms of the real signal in the neighborhood of 300 Hz emitted by a source uniformly moving along the receiving system calculated using a fast Fourier transform ("tracks" of the discrete component with a frequency of approximately 299 Hz in this case are more smeared due to the Doppler frequency shift on the signal realization length) (Fig. 5a), based on the Wigner transformation (Fig. 5b) and using linear frequency modulation compensation (Fig. 5c) as an example.

The algorithm based on linear frequency modulation compensation possesses the best noise resistance. However, for complete realization of this algorithm, it is necessary to use a priori information on the maximal frequency variation rate and assumed width of the discrete component.

In this study the F algorithm was used. For a number of technical reasons, realizations with a record length of 10 min were processed. Therefore, in the case of application of high-frequency resolution (0.001 Hz) spectral analysis algorithm it was impossible to realize in full scale its capabilities with respect to spatial source localization. These results have an estimation character.

SOME EXPERIMENTAL RESULTS

One of the main problems in the described experiment was the problem of correct determination of the noise level for the discrete component of energy supply of the ship in the neighborhood of 50 Hz on a level of a background component of similar signals generated by mechanisms that do not belong to the sea object *Sh1*.

For a frequency resolution of 0.05 Hz in the signal spectrum in the neighborhood of 50 Hz, three frequency components can be clearly seen: 49.68, 49.98, and 57.96 Hz (Fig. 6). Figure 7 shows the diagrams of angular distribution of intensity $I(\varphi)$ of acoustic power flux in the horizontal plane for these discrete components calculated for a frequency resolution of 0.2 Hz in the logarithmic scale (dB). It turned out that the discrete components with frequencies of 49.7 Hz and 57.9 Hz possess a pronounced direction toward the ship *Sh1*. For the signal with a frequency of 50 Hz, the spatial distribution of the signal is ambiguous.

Further application of high-resolution spectral analysis algorithms ($\delta f = 0.001$ Hz) yielded the conclusion that discrete components with frequencies of 49.7 Hz (49.680 Hz) and 57.9 Hz (57.961 Hz) are solitary and that with a frequency of 50.00 Hz actually consists of three closely situated components. The discrete components with average frequencies of 49.987 and 49.998 Hz are frequency-unstable, and the component with a frequency of 50.002 Hz is stable. The relatively short length of the processed signal realizations recorded in the experiment prevented precise localization of the direction of arrival of energy of these signals, but allowed the conclusion to be drawn that the first two frequency components are generated in the dock and the third is connected with noise emission by the object *Sh2*. This probably explains the complex character of the total angular intensity distri-

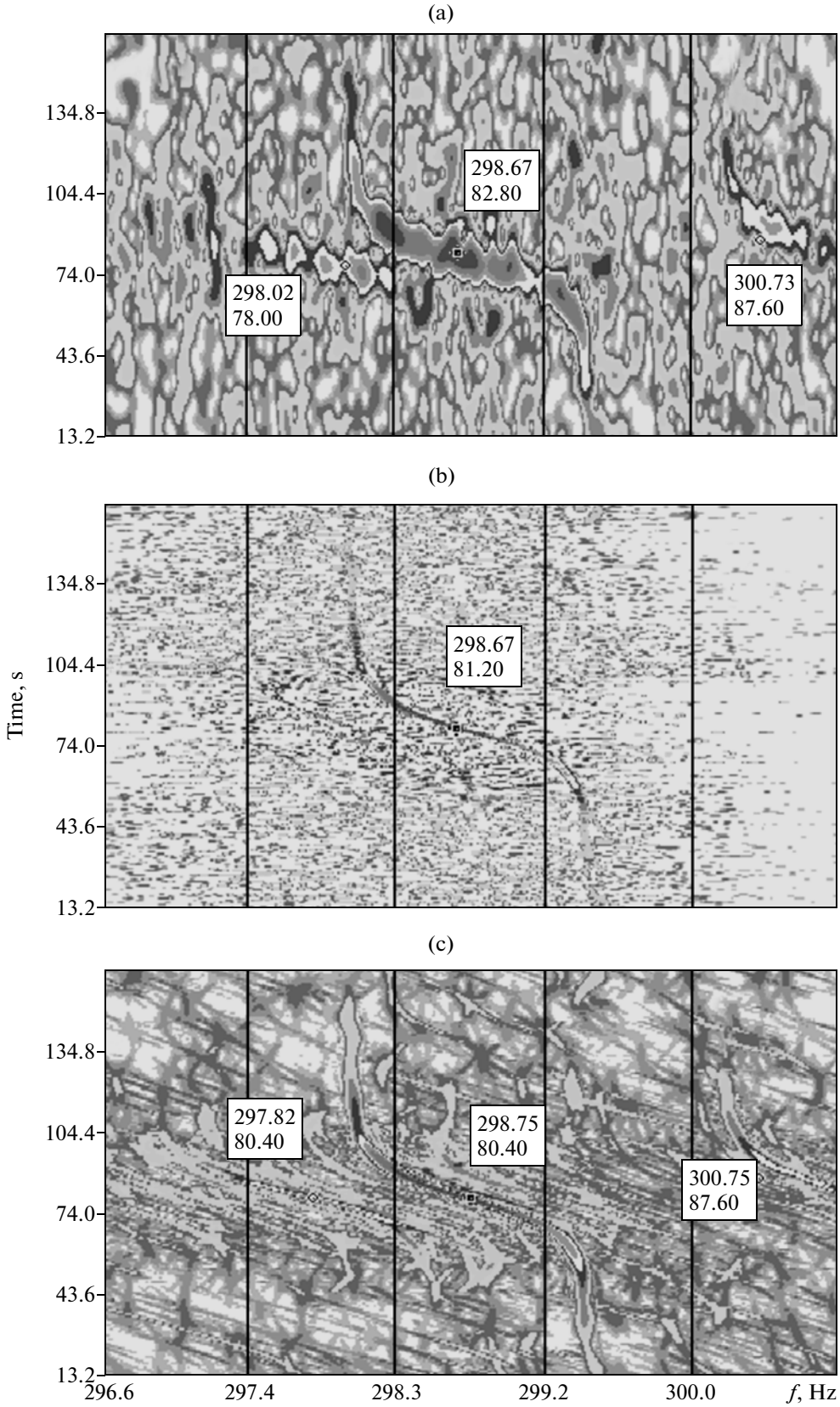

Fig. 5. Example of application of algorithms of high frequency resolution sonographic analysis for processing real signal in the neighborhood of 300 Hz from a sea object uniformly moving past the receiving system: (a) F algorithm, analysis band $\delta f = 0.06$ Hz; (b) W algorithm, $\delta f = 0.03$ Hz; (c) Q algorithm, $\delta f = 0.06$ Hz. Numbers in squares show frequency and signal level on the beam.

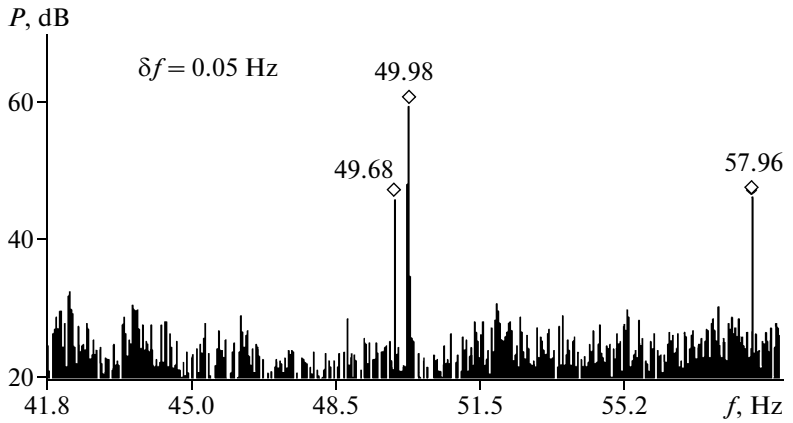

Fig. 6. Fragment of spectrum of the signal registered by acoustic pressure receiver in the neighborhood of 50 Hz for a frequency resolution of 0.05 Hz.

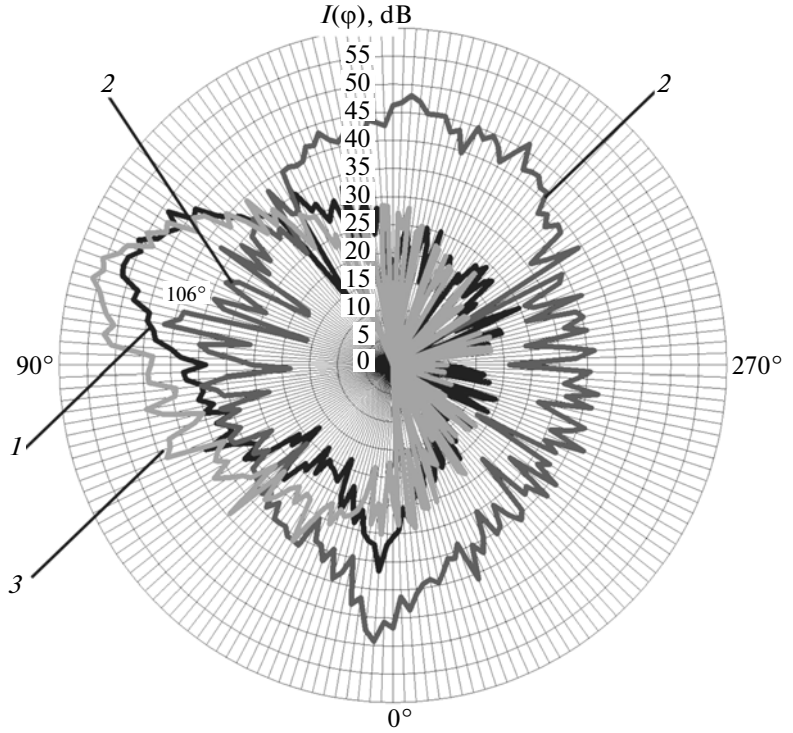

Fig. 7. Diagram of angular intensity distribution in the horizontal plane for the 0.2-Hz analysis band with central frequencies: (*1*) 49.7, (*2*) 50.0, and (*3*) 57.9 Hz. Averaging time is 500 s.

bution for these components for a frequency resolution of 0.2 Hz.

Figure 8 shows the diagrams of angular distribution of acoustic power flux intensity for 49.7 and 57.9 Hz in the vertical plane ($\delta f_i = 0.2$ Hz). The axis of the 0° diagram corresponds to the direction toward the surface. The diagram at a frequency of 49.7 Hz "points" to the source at a distance of ~23 m in the horizontal direction from the vector receiver and the diagram at a frequency of 57.9 Hz to the source at a distance of ~50 m, each within the length of the studied object *Sh1*. The presented results demonstrate the fundamental possibility of determination of the source location on the ship hull. It should be noted that the application of two spatially separated combined receiving systems makes it possible to reduce the range of uncertainty in determination of the source position.

Figure 9c shows the angular distributions in the horizontal and vertical planes for two discrete compo-

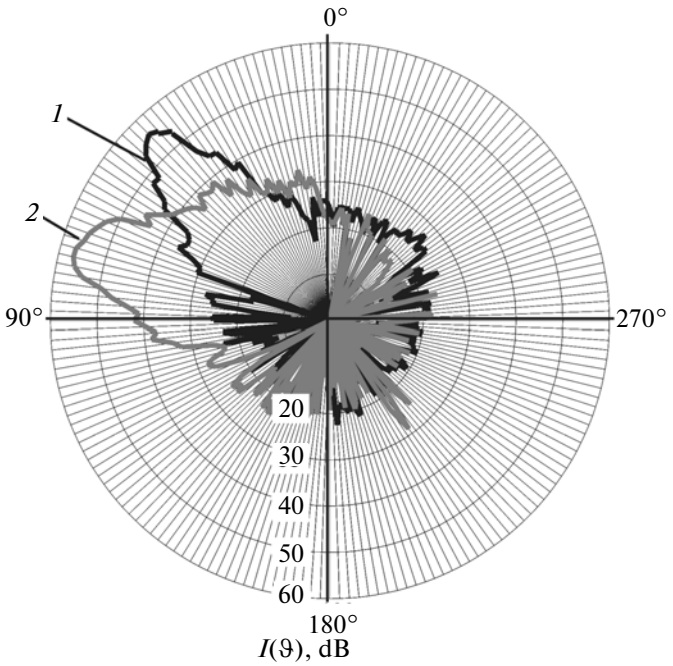

Fig. 8. Diagram of angular intensity distribution in the vertical plane for the 0.2-Hz analysis band in logarithmic scale with central frequencies: (*1*) 49.7 and (*2*) 57.9 Hz. Averaging time is 500 s.

nents of object *Sh1* with frequencies of 66.25 and 82.50 Hz for illustration. The 66.25-Hz discrete component for a frequency resolution of 0.05 Hz exceeds the background component by about 15 dB. For this component a pronounced direction toward the ship with an estimated distance of 50 m is observed. The 82.5-Hz component in the pressure channel spectrum is extremely weak; therefore, it possesses a less-pronounced direction with the same estimated distance of 50 m.

The data in Fig. 10 illustrate the capabilities of relative estimation of noise spectra of objects *Sh1* and *Sh2* in the three-octave frequency bands for spectral components with the direction to the objects *Sh1* and *Sh2*. It can be seen from this figure that these spectra essentially differ. Thus, the spectrum in the low-frequency range is mainly formed by sources of the object *Sh1*, while the spectrum in the high-frequency range, by sources situated in the direction of the object *Sh2*.

Note that these spectra of studied objects should be considered as estimation spectra only, since, in the presence of several noise sources operating in the same frequency range in the water area, they are formed by summing noise levels of discrete (or line) components. They are "separated" with respect to directions taking into account the above algorithms of statistical processing of the values of projections of the acoustic power flux vector and high-resolution spectral analysis. As regards the continuous spectrum, its level from several sources is summed in the acoustic power flux vector in a complex way. Estimating the amount and contribution of the continuum to the total noise level are a separate problem.

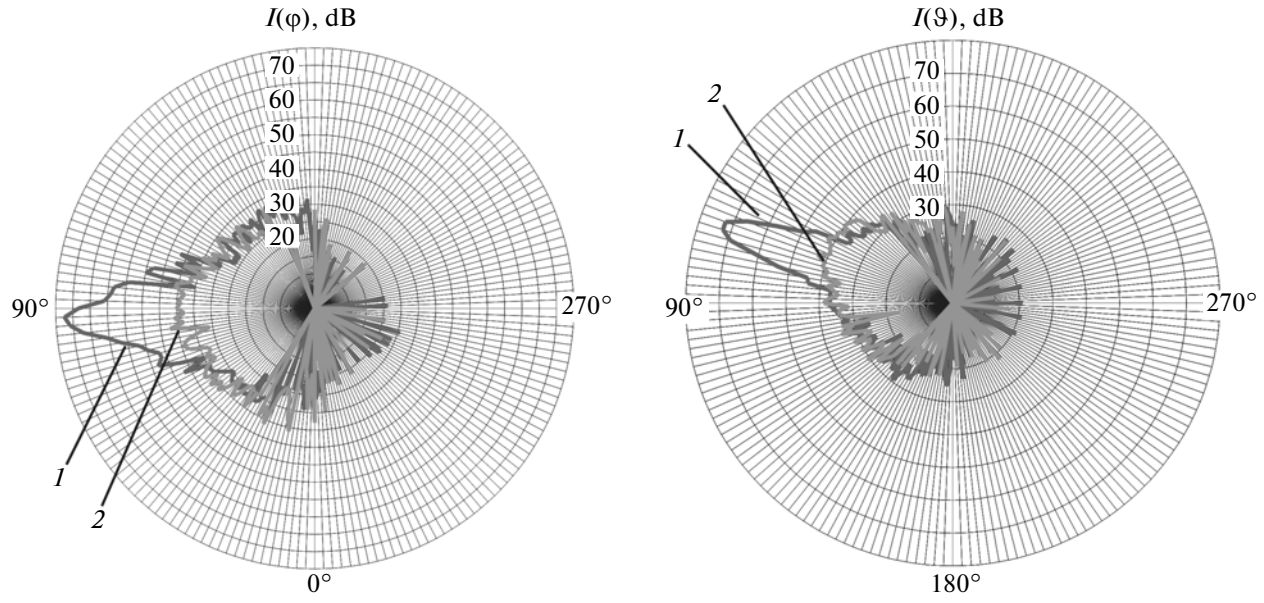

Fig. 9. Diagram of angular intensity distribution (left) in the horizontal and (right) vertical planes for the 0.2-Hz analysis band in logarithmic scale with central frequencies: (*1*) 66.25 and (*2*) 82.50 Hz. Averaging time is 500 s.

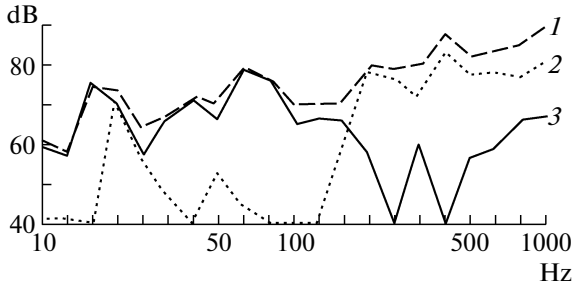

Fig. 10. Three-octave spectrum in an interval of 10–1000 Hz (*1*) from the output of acoustic pressure receiver and obtained as a result of spatial filtering of acoustic power flux vector for two objects: (*2*) *Sh2* (from the direction $\varphi \approx -114°$ and (*3*) *Sh1* (from the direction $\varphi \approx 90°$. Averaging time is 10 s.

CONCLUSIONS

Thus, the fundamental possibility of application of combined receiving systems for solution of problems of estimation of direction and localization of individual sources, source membership selection, and more reliable estimation of source noise level due to spatial signal filtering and offset from concentrated noise sources in a complex signal–noise situation of the water area was demonstrated.

REFERENCES

1. V. K. Maslov and A. M. Trokhan, Trudy VNIIFTRI **47** (139), pp. 84–131 (2004).
2. V. K. Maslov, Trudy VNIIFTRI **49** (141), 77–133 (2005).
3. Yu. I. Zakonov, P. I. Korotin, D. A. Orlov, S. P. Sazonov, A. B. Slizhov, V. I. Turchin, G. E. Fiks, and I. Sh. Fiks, Akust. Zh. **56**, 223 (2010) [Acoust. Phys. **56**, 198 (2010)].
4. V. A. Gordienko, *Vector-Phase Methods in Acoustics* (Fizmatlit, Moscow, 2007) [in Russian].
5. J.-A. Roy, in *Proceedings of the UDT Pacific 98, Feb., 1998, Sydney, Australia*, pp. 290–295.
6. J. Clark and G. Tarasek, in *Oceans'06, MTS IEEE, Revolutionize Marine Science Technology, Sept. 18–21, 2006, Hynes Convention Center, Boston, MA*.
7. V. A. Gordienko, N. V. Krasnopistsev, A. V. Nasedkin, V. N. Nekrasov, and V. N. Toropov, Acoust. Phys. **55**, 741 (2009).
8. V. A. Gordienko, E. L. Gordienko, N. V. Krasnopistsev, and V. N. Nekrasov, Akust. Zh. **54**, 774 (2008) [Acoust. Phys. **54**, 670 (2008)].
9. J. L. Pascal, Rev. Pract. Control. Dustriel **21**, 3840 (1982).
10. *Sound Intensity Analyzer Type 2134*, Instruction Manual (Bruel & Kjïer, 1983).
11. V. A. Gordienko, Ya. A. Ilyushin, and V. I. Il'ichev, Dokl. Akad. Nauk **339**, 808 (1994).
12. V. N. Toropov, in *Tomographic Methods in Physico-Technical Measurements*, Collection of Works (VNIIFTRI, Moscow, 1990), pp. 97–102 [in Russian].
13. L. Cohen, Proc. IEEE **77**, 941 (1989).
14. F. J. Harris, Proc. IEEE **66**, 60 (1978).
15. J. Max, *Methods and Technique of Signal Processing by Physical Measurements* (Mir, Moscow, 1983) [in Russian].
16. M. A. Price, *Progress in Underwater Acoustics* (Plenum, New York, 1987).